Overlap Between Anterior Cruciate Ligament and Anterolateral Meniscal Root Insertions

A Scanning Electron Microscopy Study

Brett D. Steineman,* BS, Samuel G. Moulton,† BA, Tammy L. Haut Donahue,*‡ PhD, Cristián A. Fontboté,§ MD, Christopher M. LaPrade,† BA, Tyler R. Cram,‖ MA, ATC OTC, Chase S. Dean,† MD, and Robert F. LaPrade,†‖¶ MD, PhD
Investigation performed at the Soft Tissue Mechanics Laboratory, Colorado State University, Fort Collins, Colorado, USA

Background: The anterolateral meniscal root (ALMR) has been reported to intricately insert underneath the tibial insertion of the anterior cruciate ligament (ACL). Previous studies have begun to evaluate the relationship between the insertion areas and the risk of iatrogenic injuries; however, the overlap of the insertions has yet to be quantified in the sagittal and coronal planes.

Purpose: To investigate the insertions of the human tibial ACL and ALMR using scanning electron microscopy (SEM) and to quantify the overlap of the ALMR insertion in the coronal and sagittal planes.

Study Design: Descriptive laboratory study.

Methods: Ten cadaveric knees were dissected to isolate the tibial ACL and ALMR insertions. Specimens were prepared and imaged in the coronal and sagittal planes. After imaging, fiber directions were examined to identify the insertions and used to calculate the percentage of the ACL that overlaps with the ALMR instead of inserting into bone.

Results: Four-phase insertion fibers of the tibial ACL were identified directly medial to the ALMR insertion as they attached onto the tibial plateau. The mean percentage of ACL fibers overlapping the ALMR insertion instead of inserting into subchondral bone in the coronal and sagittal planes was 41.0% ± 8.9% and 53.9% ± 4.3%, respectively. The percentage of insertion overlap in the sagittal plane was significantly higher than in the coronal plane ($P = .02$).

Conclusion: This study is the first to quantify the ACL insertion overlap of the ALMR insertion in the coronal and sagittal planes, which supplements previous literature on the insertion area overlap and iatrogenic injuries of the ALMR insertion. Future studies should determine how much damage to the ALMR insertion is acceptable to properly restore ACL function without increasing the risk for tears of the ALMR.

Clinical Relevance: Overlap of the insertion areas on the tibial plateau has been previously reported; however, the results of this study demonstrate significant overlap of the insertions superior to the insertion sites on the tibial plateau as well. These findings need to be considered when positioning for tibial tunnel creation in ACL reconstruction to avoid damage to the ALMR insertion.

Keywords: anterior cruciate ligament; ACL reconstruction; scanning electron microscopy; anterolateral meniscal root

Over the past decade, there has been an increasing emphasis on anatomic anterior cruciate ligament (ACL) reconstruction to best restore knee kinematics after an ACL tear. Although studies have shown that the position,[20] size,[15] and shape[11] of the ACL insertion site are variable, anatomic single- and double-bundle ACL reconstructions have both shown improved outcomes, especially when performed using an individualized technique.[13] However, recent investigations of anatomic ACL reconstruction have highlighted concern over iatrogenic injuries of anterior meniscal root insertions caused by reaming of tibial bone tunnels, specifically the anterolateral meniscal root (ALMR) insertion.[17,22]

While many studies have investigated the significance of the ACL and potential reconstruction techniques,[1,5,12,14,25] the complex relationship between the tibial ACL and the lateral meniscus has become a recent area of focus.[6,9,16-19,22] The ALMR insertion has been described to attach underneath the lateral portion of the ACL insertion with a disorganized fiber

The American Journal of Sports Medicine, Vol. 45, No. 2
DOI: 10.1177/0363546516666817

network connecting the 2 insertions.[9,18] An investigation of ACL reconstruction tunnel reaming demonstrated that iatrogenic injuries of the ALMR insertion area occurred in two-thirds of sample groups and that the average area of injuries was at least 25% of the original ALMR insertion area, likely because of this intricate relationship.[22] More importantly, damage to the ALMR insertion caused by tunnel reaming was found to significantly decrease its ultimate failure load.[17] Although variability in tibial ACL tunnel placement has been reported to be relatively consistent between surgeons, with 90% of tibial tunnels within applied literature-based guidelines, these studies of iatrogenic injuries suggest that even well-placed anatomic tunnels may disrupt the ALMR insertion.[23] Because the lateral meniscus has been reported to be an important secondary stabilizer of the knee, particularly during pivot-shift loading,[19] the demonstrated risk of iatrogenic injuries to the ALMR insertion during ACL reconstruction may pose a threat to overall knee integrity after this procedure.

While these studies begin to describe the complex relationship and the risk of ACL reconstruction on the ALMR insertion, further investigation of how the 2 insertions interact is necessary to understand and define the 3-dimensional relationship between these 2 structures. To further understand the quantitative anatomy of the insertion relationship, LaPrade et al[16] reported that, on average, 41% of the ACL insertion area and 63% of the ALMR insertion area overlapped with one another. Microscopic studies of the tibial insertion site have been previously conducted to investigate quantities of fibrocartilaginous zones to relate biomechanical properties of the insertion[2,3,7,8]; however, the authors are unaware of any study that has microscopically evaluated the fibrocartilaginous insertion of the tibial insertion with respect to the ALMR insertion, particularly in the sagittal and coronal planes.

Therefore, the purpose of this study was to investigate the microstructural relationship between the tibial ACL and ALMR insertions using scanning electron microscopy (SEM) in the coronal and sagittal planes. It was hypothesized that a significant portion of the ACL would overlap the ALMR insertion in both the coronal and sagittal planes.

METHODS

Specimen Preparation

Institutional review board approval was obtained for this study (Colorado State University 14-5240H). A total of 10 fresh-frozen human cadaveric knees from 5 male and 5 female specimens were used with a mean age of 52.7 years (range, 33-63 years) and mean body mass index of 22.4 kg/m^2 (range, 15-34 kg/m^2), and knees that displayed macroscopic degenerative changes or evidence of trauma, such as osteoarthritis, meniscal tears, or ligament injuries, were excluded. Specimens were dissected to remove all soft tissues around the knee, including the collateral ligaments and the posterior cruciate ligament. Care was taken to isolate and preserve the entire ACL and ALMR insertions throughout dissection. The midsubstance of the ACL was then transected to separate the femoral and tibial insertions. Once separated, the proximal tibias were transected 20 mm from the articular cartilage surface using an oscillating saw. A bone saw was then used to remove the excess tibial plateau and create a 30 × 30 × 20–mm rectangular block encompassing the tibial ACL and ALMR insertions (Figure 1).

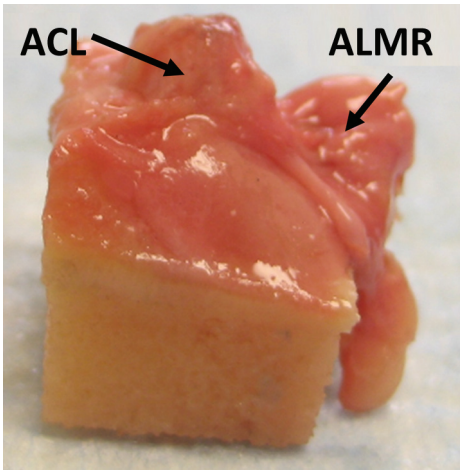

Figure 1. Sample photograph of the rectangular bone block cut to include the tibial anterior cruciate ligament (ACL) and anterolateral meniscal root (ALMR) insertions.

Samples were prepared for SEM similar to previously presented methods.[21,24] Briefly, the samples were placed in fixative (2.5% glutaraldehyde) for 48 hours at room temperature. The samples were then submerged in 10% formic acid to decalcify at room temperature. After decalcification, the samples were immersed in a 1% tannic acid solution buffered with 0.05 M cacodylate (pH 7.2) for 4 hours and then rinsed in distilled water for 24 hours. Samples were then dehydrated in ascending concentrations of ethanol (30%, 50%, 70%, 80%, 90%, and 100%) for 10 minutes each and cut into 2-mm sections. The number of sections

¶Address correspondence to Robert F. LaPrade, MD, PhD, Steadman Philippon Research Institute, 181 West Meadow Drive, Suite 1000, Vail, CO 81657, USA (email: drlaprade@sprivail.org).
*School of Biomedical Engineering, Colorado State University, Fort Collins, Colorado, USA.
†Steadman Philippon Research Institute, Vail, Colorado, USA.
‡Department of Mechanical Engineering, Colorado State University, Fort Collins, Colorado, USA.
§Department of Orthopaedic Surgery, Pontificia Universidad Católica de Chile, Santiago, Chile.
‖The Steadman Clinic, Vail, Colorado, USA.
One or more of the authors has declared the following potential conflict of interest or source of funding: R.F.L. receives royalties from Arthrex Inc and Smith & Nephew; is a paid consultant for Arthrex Inc, Ossur, and Smith & Nephew; and receives research support from Arthrex Inc, Smith & Nephew, Ossur, and Linvatec.

ranged from 5 to 7 sections per specimen. Samples from 5 specimens were cut into coronal sections with the ALMR insertion fibers running approximately parallel to the section plane, and samples from the remaining 5 specimens were cut into sagittal sections with the ACL fibers running approximately parallel to the section plane. Once sectioned, the samples were placed in ascending concentrations of hexamethyldisilazane for 10 minutes each. The samples were then dried and stored in a vacuum desiccator.

Imaging

Samples were mounted onto a stub with conductive double-sided tape and copper tape with the surface of interest facing up toward the electron beam. The samples were then coated with 10 nm gold and scanned with a scanning electron microscope (JEOL USA Inc) in the secondary electron emission mode with an accelerating voltage of 15 kV.

To evaluate the relationship between the tibial ACL insertion and the ALMR insertion in the coronal plane, a section from each specimen was taken from the middle of the ALMR insertion to image. A section from each specimen used for viewing the sagittal plane was taken closer to the lateral side of the ACL insertion to incorporate the ALMR insertion. Section locations were chosen to evaluate the maximum overlap of the ACL and ALMR insertions. Each section was assessed at high magnification (up to 1500×) to view individual insertion fibers. SEM allowed real-time imaging of sections with the availability to maneuver around the sections at high magnifications; thus, these high-resolution images were used to identify the entirety of both insertions and observe where they overlap. The 4-phase fibers of the tibial ACL insertion were evaluated with respect to the ALMR insertion fibers. Fibrocartilaginous entheses have been previously described as 4 distinct zones: zone 1 consists of dense, fibrous connective tissue; zone 2 consists of uncalcified fibrocartilage; zone 3 consists of calcified fibrocartilage; and zone 4 consists of subchondral bone.[2,4,24] Approximately 15 to 20 lower magnification (15×) images were then taken using the built-in SEM camera across the entirety of each sample and stitched together for quantitative analysis of the insertion relationship using ImageJ software (National Institutes of Health).

Data Analysis

The percentage of the tibial ACL insertion that overlapped with the ALMR insertion instead of inserting into subchondral bone was determined in each plane to further understand the relationship between the 2 insertions. For each sample, the length of the ACL insertion that visibly inserted into subchondral bone was initially determined by measuring the boundary between the ligament-bone interface of the 2-phase insertion fibers and tidemark of the 4-phase insertion fibers described in previous literature.[2,4,24] The length of the ACL insertion that overlapped with the ALMR insertion was determined using the high-magnification images. The percentage of the ACL insertion that overlapped with the ALMR insertion fibers instead of inserting into subchondral bone was then calculated for each sample. Measurements were taken by 2 raters from the stitched SEM images using ImageJ software.

A 2-sample, equal-variance Student t test was performed on the percentages of insertion interaction between the coronal and sagittal sections. Statistical significance was determined to be present for $P < .05$. Additionally, interrater intraclass correlation coefficients (ICCs) were calculated to test the reliability of measurements between the 2 raters. Measurements were also taken again after 2 weeks to calculate the intrarater ICCs and determine the reliability between measurements repeated by a single rater.

RESULTS

Macroscopic Appearance

The ACL tibial insertion had a fan-like appearance macroscopically and was located posteromedial to the ALMR insertion. In all 10 specimens, the ALMR inserted underneath the lateral portion of the ACL. The relationship of the ACL tibial insertion and the ALMR insertion was visible upon forming the coronal and sagittal sections. On the coronal sections, the ALMR insertion fibers clearly coursed under the lateral portion of the tibial ACL insertion. On the sagittal sections, the ALMR insertion fibers were visible inferior to the ACL insertion fibers on sections from the lateral portion of the ACL tibial insertion but were not visible or present on sections from the central or medial portion.

Microscopic Appearance

The tibial ACL insertion displayed an intimate relationship with the ALMR insertion as both structures transitioned into bone in both the sagittal and coronal sections. The ALMR insertion fibers were distinguished from the ACL fibers in the SEM images by the difference in orientation at high magnification. Initially, at low magnification, each section was viewed, and the region of overlap in the coronal (Figure 2) and sagittal (Figure 3) planes was identified to investigate further at higher magnification. With increasing magnification, the individual fibers became more easily distinguishable, and the orientations of individual fibers of the ACL and ALMR insertions were identified. For all coronal sections, the ACL insertion fibers appeared to run vertically in and out of the image (Figure 4A). The ALMR insertion fibers ran in a diagonal orientation along the plane of view as they approached the bone interface (Figure 4B). For all sagittal sections, the appearance of the fibers in SEM images was reversed. The ACL insertion fibers ran diagonally along the plane of view, while the ALMR insertion fibers appeared to run vertically in and out of the image (Figure 5). Once the separate insertions were identified, the overlap was mapped across each image (Figure 3). Additionally, 4-phase fibers of the tibial ACL were found medially adjacent to the ALMR insertion in the coronal plane (Figure 2). The 4-phase insertion

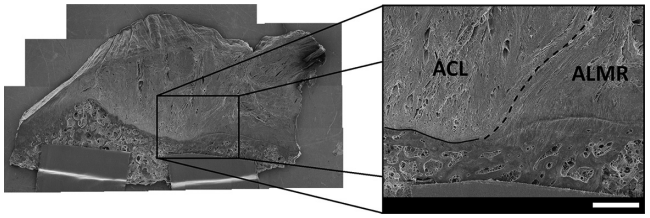

Figure 2. Scanning electron microscopy image of the intricate relationship between the 2 insertions in the coronal plane. Note the 4-phase insertion fibers of the anterior cruciate ligament (ACL) with the tidemark (solid line) separating the uncalcified fibrocartilage layer from the calcified fibrocartilage layer directly adjacent to the anterolateral meniscal root (ALMR) insertion. The dashed line represents the interaction between the ACL and ALMR. (Close-up image: 15×; working distance = 25 mm; scale bar = 1 mm).

fibers of the ACL were not clearly visible or not present in the sagittal sections imaged.

After the insertions of the tibial ACL and ALMR were identified, the percentage of the ACL insertion overlapping the ALMR insertion was calculated for each section in both planes. The combined interrater ICC was 0.81 for all measurement values, with interrater ICCs of 0.78 and 0.84 for measurements of coronal and sagittal sections, respectively. The intrarater ICC was 0.98 for all measurements, with intrarater ICCs of 0.98 and 0.95 for measurements of coronal and sagittal sections, respectively. For the coronal sections, the tibial ACL insertion overlapped the ALMR insertion with a mean percentage of 41.0% ± 8.9% (Table 1). The mean length of the measured overlap between the 2 insertions in the coronal plane was 6.5 ± 1.9 mm, while the mean length of the measured interaction between the ACL insertion and subchondral bone was 9.2 ± 1.4 mm (Table 1). For the sagittal sections, the tibial ACL insertion overlapped the ALMR insertion with a mean percentage of 53.9% ± 4.3% (Table 2). The mean length of the measured overlap between the 2 insertions in the sagittal plane was 9.5 ± 2.0 mm, while the mean length of the measured interaction between the ACL insertion and subchondral bone was 8.3 ± 2.8 mm (Table 2). The percentage of insertion overlap in the sagittal plane was significantly higher than in the coronal plane ($P = .02$).

DISCUSSION

The purpose of this study was to microscopically investigate and quantify the overlap between the tibial ACL and ALMR insertions using SEM in the coronal and sagittal planes. The results of the investigation support our hypothesis that a significant portion of the tibial ACL insertion overlaps the ALMR insertion in both the coronal and sagittal planes. Our investigation showed that, on average, 41.0% of the ACL insertion overlaps the ALMR insertion in the coronal plane and 53.9% in the sagittal plane. Although only a single section was viewed for each specimen, the imaged sections were selected to represent the maximum

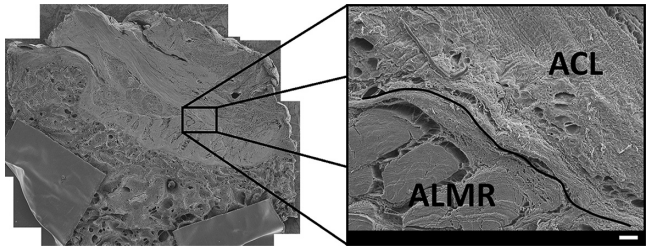

Figure 3. Scanning electron microscopy image of the intricate relationship between the 2 insertions in the sagittal plane. The solid line represents where the anterior cruciate ligament (ACL) insertion overlaps the anterolateral meniscal root (ALMR) insertion within the plane of view. 15×; working distance = 25 mm. (Close-up image: 75×; working distance = 10 mm; scale bar = 100 μm).

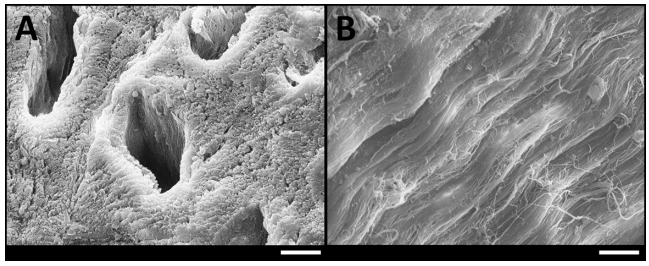

Figure 4. Scanning electron microscopy images of the (A) tibial anterior cruciate ligament (ACL) insertion fibers and the (B) anterolateral meniscal root (ALMR) insertion fibers taken of a coronal section. Note that the ACL fibers appear to run vertically in and out of the image while the ALMR fibers run along the image plane. 1500×; working distance = 10 mm; scale bars = 10 μm.

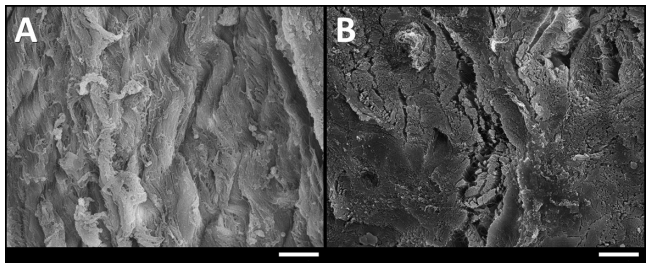

Figure 5. Scanning electron microscopy images of the (A) tibial anterior cruciate ligament (ACL) insertion fibers and the (B) anterolateral meniscal root (ALMR) insertion fibers taken of a sagittal section. Note that the ACL fibers appear to run along the image plane while the ALMR fibers run vertically in and out of the image. 1500×; working distance = 10 mm; scale bars = 10 μm.

overlap of the tibial ACL insertion in the 2 planes of interest. Previously, a measurement of ACL-ALMR overlap in the transverse plane, described as insertion areas on the tibial plateau, was conducted.[16] That study measured the

TABLE 1
Average Measurements of 2 Raters for Each Specimen Used to Calculate the Overlap of the ACL and ALMR Insertions Within the Coronal Plane[a]

	Coronal Sections (Superior-Inferior and Medial-Lateral Plane)		
	ACL-ALMR, mm	ACL-Bone, mm	ACL-ALMR Overlap, %
Specimen 1	8.2	9.0	47.7
Specimen 2	3.6	10.3	25.9
Specimen 3	7.5	10.9	40.8
Specimen 4	7.4	8.4	46.8
Specimen 5	5.7	7.3	43.8
Mean (95% CI)	6.5 (4.2-8.8)	9.2 (7.4-11.0)	41.0 (30.0-52.0)

[a]ACL-ALMR, length of measurement that ACL overlaps with ALMR instead of inserting into subchondral bone; ACL-Bone, length of measurement that ACL inserts into subchondral bone; ACL-ALMR Overlap, percentage that the ACL overlaps with the ALMR instead of inserting into subchondral bone. ACL, anterior cruciate ligament; ALMR, anterolateral meniscal root.

TABLE 2
Average Measurements of 2 Raters for Each Specimen Used to Calculate the Overlap of the ACL and ALMR Insertions Within the Sagittal Plane[a]

	Sagittal Sections (Superior-Inferior and Anterior-Posterior Plane)		
	ACL-ALMR, mm	ACL-Bone, mm	ACL-ALMR Overlap, %
Specimen 6	8.3	8.0	51.0
Specimen 7	7.7	6.5	54.2
Specimen 8	8.0	5.2	60.6
Specimen 9	11.1	9.4	54.1
Specimen 10	12.2	12.5	49.4
Mean (95% CI)	9.5 (6.9-12.0)	8.3 (4.8-11.8)	53.9 (48.6-59.2)

[a]ACL-ALMR, length of measurement that ACL overlaps with ALMR instead of inserting into subchondral bone; ACL-Bone, length of measurement that ACL inserts into subchondral bone; ACL-ALMR Overlap, percentage that the ACL overlaps with the ALMR instead of inserting into subchondral bone. ACL, anterior cruciate ligament; ALMR, anterolateral meniscal root.

entire area of both the tibial ACL and ALMR insertions on the tibial plateau using a coordinate measuring device and demonstrated that an average of 41% of the ACL insertion area overlapped the ALMR insertion. The present study supplements previous knowledge of the overlap by providing information of the additional 2 anatomic planes. In combination, the 2 studies show that the tibial ACL overlaps the ALMR insertion by at least 40%, on average, in all 3 anatomic planes with the greatest overlap found in the sagittal plane.

The additional information regarding the anterior horn of the lateral meniscus and its intimate relationship with the tibial ACL insertion may have important clinical implications. Although there are no case reports of ALMR avulsions due to bone tunnel drilling, previous studies have demonstrated a clinical risk of iatrogenic injuries to the ALMR insertion.[17,22] Most notably, anatomically placed tibial tunnels for ACL reconstruction have been reported to lead to damage of a significant portion of the ALMR insertion area and to significantly decrease the insertion failure load.[17] This study utilized an 11 mm–diameter reamer, which is larger than the 9 mm–diameter reamer commonly used during hamstring ACL reconstruction techniques; however, an 11 mm–diameter reamer is often used for bone-tendon-bone grafts and reconstructions in young and active populations. Therefore, the previous study may not represent the results of all ACL reconstruction procedures, but it does represent a larger diameter reamer used in some ACL reconstructions. Additionally, this study reported that all failures of the ALMR insertion were caused by bony avulsions. The authors also mentioned that the bony avulsions in their study were not necessarily consistent clinically, so the bony avulsion failures may have been an intrinsic result of their testing procedure. Although this study did not demonstrate complete tears from the tibial plateau as failures, it did find that failure was caused by ALMR insertion disruption by tunnel reaming.

Another study utilized a 10 mm–diameter reamer to create anatomically placed tibial tunnels using a tibial aiming device set at 2 different angles of 40° and 60°.[22] That study reported iatrogenic damage to 29% and 26% of the ALMR insertion area for the 40° and 60° groups, respectively. This study utilized a 10 mm–diameter reamer, which as previously stated is larger than the 9 mm–diameter reamer used for some ACL reconstructions; however, a 10 mm–diameter reamer is in the range of common clinically used reamers. Additionally, this study demonstrated significant anterior translation of the reamed tunnel center from the native ACL insertion area. Although this translation may have contributed to

an increase in iatrogenic injuries to the ALMR insertion, the authors utilized a precise measurement technique to determine appropriate tunnel locations. Because the cadaveric joints were open and the femur removed, the tunnel site was accurately located. Therefore, the authors believed that this translation might be an intrinsic risk for reaming the tibial tunnels during ACL reconstruction. The significance of the amount of ALMR insertion damage caused by tunnel reaming has not yet been quantified; however, these studies have demonstrated the clinical risk of iatrogenic injuries to the ALMR insertion involved with even properly placed tibial tunnels.

The results from the present study supplement previous knowledge of insertion overlap and the risk of iatrogenic injuries. Primarily, this study was the first to quantify the ACL insertion overlap of the ALMR insertion in the coronal and sagittal planes. Overlap of the insertion areas on the tibial plateau has been previously reported; however, the results of this study demonstrate significant overlap of the insertions superior to the insertion sites on the tibial plateau as well. The results of the present study in addition to the iatrogenic injury studies may suggest that the angle of the guide contributes to the amount of ALMR insertion fibers that are disrupted. Although these studies have used the insertion area as an outcome variable, the guide angle may cause damage to the further superior fibers of the insertion even if the insertion area is not disrupted because of this significant overlap in the coronal and sagittal planes. Again, the clinically significant amount of disruption in the ALMR insertion, whether of the insertion area or the insertion fibers superior to the tibial plateau surface, has yet to be defined. Future studies should be conducted to determine how much damage to the ALMR insertion is acceptable to properly restore ACL function without increasing the risk for tears of the ALMR.

Additionally, 4-phase insertion fibers consisting of dense, fibrous connective tissue; uncalcified fibrocartilage; calcified fibrocartilage; and subchondral bone zones were identified in the ACL insertion medially adjacent to ALMR insertion fibers in the central coronal plane.[2,24] The 4-phase insertion fibers were not present or identifiable in images where the ACL overlapped the ALMR insertion in the sagittal plane because these sections were taken from the furthest lateral side of the ACL and these superficial portions are frequently more fibrous.[4] While it has been believed that a main goal during ACL reconstruction should be to place a tunnel within the center of the 4-phase insertion fibers, described as the most structurally important insertion fibers,[10] this study found that 4-phase insertion fibers of the tibial ACL were found medial to the overlap with the ALMR. This intricate relationship and overlap theoretically complicate the placement of a tibial tunnel for ACL reconstruction. These structurally important fibers that insert adjacent to the ALMR insertion need to be accounted for during ACL reconstruction. The risk of iatrogenic injuries to the ALMR fibers has previously been discussed; however, the clinically significant amount of ALMR insertion disruption has yet to be defined. Therefore, further investigation of the tibial ACL 4-phase insertion fibers with respect to the location of the ALMR insertion fibers is warranted to determine how much damage to the ALMR insertion is clinically acceptable during ACL reconstruction.

We also recognize that this study has limitations. The analysis was limited to 10 total specimens. Although the shape of the insertions varied among specimens, overlap between the tibial ACL and ALMR insertions was present in all 10 specimens. Additionally, the shape of the tibial insertion site has been shown to vary among 3 common patterns, and this study did not identify the shapes of the insertion sites for the specimens.[11] How the tibial insertion site pattern affects the overlap of the ALMR insertion is unknown; therefore, the tibial insertion pattern may have caused variability in the overlap measured. The overlapping relationship with respect to the different tibial insertion sites should be investigated to further understand this relationship and how it affects ACL reconstruction.

CONCLUSION

This study demonstrated significant overlap of the ALMR insertion by the tibial ACL insertion in the coronal and sagittal planes and supplements a previous study's evaluation of the overlapping relationship insertion areas. As the ACL inserted into tibial subchondral bone, the lateral portion of the ACL overlapped the ALMR insertion in both the coronal and sagittal planes, on average, by 41.0% and 53.9%, respectively. Previous studies showing iatrogenic damage to the ALMR insertion and the results of this study illustrate the intricacy of this relationship, and further studies should determine what amount of ALMR insertion disruption is acceptable for a clinically successful ACL reconstruction procedure.

ACKNOWLEDGMENT

The authors acknowledge Grant J. Dornan, MSc, for statistical guidance and calculations.

REFERENCES

1. Arnoczky SP. Anatomy of the anterior cruciate ligament. *Clin Orthop Relat Res*. 1983;172:19-25.
2. Beaulieu ML, Carey GE, Schlecht SH, et al. Quantitative comparison of the microscopic anatomy of the human ACL femoral and tibial entheses. *J Orthop Res*. 2015;33(12):1811-1817.
3. Benjamin M, Evans EJ, Rao RD, et al. Quantitative differences in the histology of the attachment zones of the meniscal horns in the knee joint of man. *J Anat*. 1991;177:127-134.
4. Benjamin M, Kumai T, Milz S, et al. The skeletal attachment of tendons-tendon ''entheses.'' *Comp Biochem Physiol A Mol Integr Physiol*. 2002;133(4):931-945.
5. Edwards A, Bull AM, Amis AA. The attachments of the anteromedial and posterolateral fibre bundles of the anterior cruciate ligament, part 1: tibial attachment. *Knee Surg Sports Traumatol Arthrosc*. 2007;15(12):1414-1421.
6. Ellman MB, LaPrade CM, Smith SD, et al. Structural properties of the meniscal roots. *Am J Sports Med*. 2014;42(8):1881-1887.
7. Evans EJ, Benjamin M, Pemberton DJ. Fibrocartilage in the attachment zones of the quadriceps tendon and patellar ligament of man. *J Anat*. 1990;171:155-162.

8. Evans EJ, Benjamin M, Pemberton DJ. Variations in the amount of calcified tissue at the attachments of the quadriceps tendon and patellar ligament in man. *J Anat*. 1991;174:145-151.
9. Furumatsu T, Kodama Y, Maehara A, et al. The anterior cruciate ligament-lateral meniscus complex: a histological study. *Connect Tissue Res*. 2016;57(2):91-98.
10. Gao J, Messner K. Quantitative comparison of soft tissue-bone interface at chondral ligament insertions in the rabbit knee joint. *J Anat*. 1996;188(Pt 2):367-373.
11. Guenther D, Irarrázaval S, Nishizawa Y, et al. Variation in the shape of the tibial insertion site of the anterior cruciate ligament: classification is required [published online December 12, 2015]. *Knee Surg Sports Traumatol Arthrosc*. doi:10.1007/s00167-015-3891-2.
12. Harner CD, Baek GH, Vogrin TM, Carlin GJ, Kashiwaguchi S, Woo SL. Quantitative analysis of human cruciate ligament insertions. *Arthroscopy*. 1999;15(7):741-749.
13. Hussein M, van Eck CF, Cretnik A, et al. Individualized anterior cruciate ligament surgery: a prospective study comparing anatomic single- and double-bundle reconstruction. *Am J Sports Med*. 2012;40(8):1781-1788.
14. Kopf S, Musahl V, Tashman S, Szczodry M, Shen W, Fu FH. A systematic review of the femoral origin and tibial insertion morphology of the ACL. *Knee Surg Sports Traumatol Arthrosc*. 2009;17(3):213-219.
15. Kopf S, Pombo MW, Szczodry M, et al. Size variability of the human anterior cruciate ligament insertion sites. *Am J Sports Med*. 2011;39(1):108-113.
16. LaPrade CM, Ellman MB, Rasmussen MT, et al. Anatomy of the anterior root attachments of the medial and lateral menisci: a quantitative analysis. *Am J Sports Med*. 2014;42(10):2386-2392.
17. LaPrade CM, Smith SD, Rasmussen MT, et al. Consequences of tibial tunnel reaming on the meniscal roots during cruciate ligament reconstruction in a cadaveric model, part 1: the anterior cruciate ligament. *Am J Sports Med*. 2015;43(1):200-206.
18. Seibold R, Shuhmacher P, Fernandez F, et al. Flat midsubstance of the anterior cruciate ligament with tibial ''C''-shaped insertion site. *Knee Surg Sports Traumatol Arthrosc*. 2015;23(11):3136-3142.
19. Shybut TB, Vega CE, Haddad J, et al. Effect of lateral meniscal root tear on the stability of the anterior cruciate ligament-deficient knee. *Am J Sports Med*. 2015;43(4):905-911.
20. Takahashi M, Doi M, Abe M, et al. Anatomical study of the femoral and tibial insertions of the anteromedial and posterolateral bundles of human anterior cruciate ligament. *Am J Sports Med*. 2006;34(5):787-792.
21. Villegas DF, Haut Donahue TL. Collagen morphology in human meniscal attachments: a SEM study. *Connect Tissue Res*. 2010;51(5):327-336.
22. Watson JN, Wilson KJ, LaPrade CM, et al. Iatrogenic injury of the anterior meniscal root attachments following anterior cruciate ligament reconstruction tunnel reaming. *Knee Surg Sports Traumatol Arthrosc*. 2014;23(8):2360-2366.
23. Wolf BR, Ramme AJ, Wright RW, et al. Variability in ACL tunnel placement: observational clinical study of surgeon ACL tunnel variability. *Am J Sports Med*. 2013;41(6):1265-1273.
24. Zhao L, Thambyah A, Broom ND. A multi-scale structural study of the porcine anterior cruciate ligament tibial enthesis. *J Anat*. 2014;224(6):624-633.
25. Ziegler CG, Pietrini SD, Westerhaus BD, et al. Arthroscopically pertinent landmarks for tunnel positioning in single-bundle and double-bundle anterior cruciate ligament reconstructions. *Am J Sports Med*. 2011;39(4):743-752.